JOURNAL OF MECHANICAL ENGINEERING AND SCIENCES
ISSN: 2289-4659 e-ISSN: 2231-8380
VOLUME 18, ISSUE 1, 2024, 9898 – 9908
DOI: https://doi.org/10.15282/jmes.18.1.2024.8.0783

UNIVERSITI MALAYSIA PAHANG AL-SULTAN ABDULLAH

RESEARCH ARTICLE

Effect of substrate's surface roughness on corrosion and wear rate of Ni-GO nanocomposite coating

N. S. Yussoff[1], N. R. N. Roseley[1]*, N. H. Saad[1], A. R. Bushroa[2], J. K. Katiyar[3]

[1] School of Mechanical Engineering, Universiti Teknologi MARA, 40450 Shah Alam, Selangor, Malaysia
Phone: +603-5543 5161
[2] Centre of Advanced Manufacturing and Materials Processing (AMMP), Department of Mechanical Engineering, University of Malaya, 50603 Kuala Lumpur, Malaysia
[3] Department of Mechanical Engineering, SRM Institute of Science and Technology, Kattankulathur, Chennai-603203, Tamil Nadu, India

ABSTRACT - Corrosion is a natural process that occurs when refined metal is converted into a more stable form, such as oxide, hydroxide, or sulfide. Wear is the failure of a surface due to dynamic contact between two surfaces. In offshore operations and environments, corrosion and wear are major problems due to the presence of corrosive and abrasive elements. The coating is a common surface protection method that enhances corrosion resistance and prolongs lifespan. In this work, a Ni-Graphene nanocomposite coating was fabricated using the electrodeposition method. This work aimed to fabricate a Ni-GO nanocomposite coating on mild steel with different surface roughness, to characterize the physical, mechanical, and chemical properties of the coating, and to investigate its corrosion and wear rate. The fabrication process involved preparing substrates coated with Ni-GO nanocomposite through a 45-minute constant current electrodeposition process. The coated specimens were characterized using X-ray diffraction machine, scanning electron microscope, Alicona infinite focus, vicker's hardness test, raman spectroscopy, and adhesion test. The corrosion and wear rate of the coatings were investigated using a slurry erosion tester and salt water spray, respectively. The results showed that the Ni-GO nanocomposite coating on a smooth surface roughness substrate achieved the highest microhardness, wear resistance, and corrosion resistance, with values of 468.8 HV, 0.182 % weight loss, and 0.03 % weight gain, respectively. This indicates that the specimen coated with a smooth surface roughness substrate provided better coating performance than the rough and medium surface roughness substrates.

ARTICLE HISTORY
Received : 04th Oct. 2023
Revised : 03rd Jan. 2024
Accepted : 12th Jan.. 2024
Published : 30th Mar. 2024

KEYWORDS
Surface roughness
Nanocomposite coating
Corrosion
Wear

1. INTRODUCTION

Corrosion is an inevitable and undesirable process that occurs when metal frequently reacts with its surrounding environment, affected by factors such as humidity and temperature. While this phenomenon is a regular part of daily life, the demand for anti-corrosion coatings in various industries including construction, automotive, transportation, consumer goods, and industrial machinery is growing due to increasing end-user requirements [1]. Multiple studies have demonstrated that dense oxide films on metal and alloy surfaces protect the substrates from corrosive environments with their effectiveness depending on higher surface roughness. Wasiu et al. [2] discussed how differences between experimental and analytical data can rarely influence corrosion behavior due to various interacting factors. The main category influencing the electrochemical or mechanical behavior of the coated surface was found according to substrate surface conditions. However, the varied interactions of the coating layer on different substrate surfaces still affect the corrosion rate. Yu et al. [3] presented the investigating ways to lessen the possibility of corrosion in daily settings. A traditional anti-corrosion strategy that includes cathodic protection, corrosion inhibitors, and corrosion-resistant alloy, all of which are successful in lowering the risk of corrosion in particular environments. As a result, it may be possible to create an anti-corrosion coating for carbon steel surfaces that strikes a compromise between cost and corrosion protection, making it a practical choice for wider use in the system under study. From this vantage point, electroless Ni-P coating has proven useful in a variety of settings due to its exceptional corrosion resistance, advantageous mechanical qualities, and simple manufacturing procedure. Yuri et al. [4] reported the most universal strategy to prevent metal from corrosion is organic coating (OC). It is because of its significant reliability and simplicity of application. Based on the study, to obtain a good comprehensive performance for instance physical barrier, corrosion resistance, and electrical and thermal conductivities, pure OC systems have lacked and are unable to resolve it. Therefore, a remarkable incorporation of graphene in polymer or metal matrix should be implemented to improve multiple OCs' corrosion protection.

Moreover, to enhance the corrosion resistance in the coated layer, the incorporation of graphene into the metal matrix of the composite was implemented. Graphene is a two-dimensional hexagonal lattice structure consisting of a single layer of carbon atoms and experiences unique mechanical and electrothermal properties resulting in several works. It's usually being used as an additive with metal matrix to benefit higher performance for surface protection purposes [5]. Besides,

***CORRESPONDING AUTHOR | N. R. N. Roseley** | ✉ roselina_roseley@uitm.edu.my

nickel was extensively studied and considered to be a crucial deposit, exhibiting unique features of high density, minimum porosity, and excellent corrosion resistance when incorporated with inert particles via electrodeposition. Both nickel and graphene are novel materials that can be employed for corrosion resistance [6]. The use of a nanocrystalline layer has been claimed to enhance corrosion and wear resistance, thereby extending the durability of machinery and tribology applications. On the other hand, the noteworthy incorporation of Ni-Graphene (Ni-GO) results in reduced maintenance costs and fewer occurrences of machinery malfunctions for organizations. Raghupathy et al. [7] reported the effect of graphene oxide as a unique material that has significantly attracted attention for corrosion inhibition. Consequently, the ultrathin graphene layer in the Cu-GO composite coating has proven effective in protecting the underlying metal from corrosion. Zhe Duan [8] carried out a study on the use of single-layer defect-free graphene to prevent metal corrosion. Graphene exhibits superior shielding properties and functions as a corrosion inhibitor by preventing moisture and oxygen molecules from penetrating the metal matrix's surface. On the other hand, the utilization of graphene in preventing metal corrosion is still in its early stages and encounters multiple barriers. Also, the preparation of a graphene layer with imperfection and well-dispersed polymer resin using a non-covalent bond remains unresolved.

Another study of Ni-Graphene nanocomposite coating on carbon steel substrates for anti-corrosion applications has shown substantial enhancements in both microhardness and corrosion resistance. The distinctive properties of graphene have led to numerous reports on nanocomposite coatings utilizing it. These coatings are often applied for surface protection and anti-corrosion functions [9, 10]. Ni-Graphene composite coatings on carbon steel substrates have been developed for anti-corrosion purposes, showing significant improvements in both microhardness and corrosion resistance. The application of a Ni-GO nanocomposite coating is believed to enhance the materials' wear and corrosion resistance capabilities. However, the lack of design cost-effective and efficient coating solution anticipates enhancing the corrosion resistance and wearability of mild steel in offshore environments maintaining its microhardness and adhesion properties, using a Ni-GO nanocomposite coating with optimized surface roughness levels [11]. Therefore, this work aims to optimize surface roughness levels and examine the characteristics, wear, and corrosion behavior of the Ni-GO coating. A comprehensive investigation of the coatings was carried out in morphology, microhardness, and surface roughness, as well as the concentration of nickel and graphene in the coating.

2. MATERIALS AND METHODS

2.1 Material and Electrolyte Preparation

In this study, mild steel was used as the substrate. The substrate was designed in a rectangular shape with a consistent size of 76 mm x 25 mm x 4 mm for all samples, complying with the standard for the slurry erosion testing machine. The substrate underwent cleaning to remove oxide layers, followed by categorization into three groups based on different grit values of grid sandpaper, resulting in three distinct surface roughness levels. Table 1 provides details on the types of flap disks used in substrate preparation. The 'rough' parameter was achieved using flap disks with grit values of #120 and #180, while the 'medium' parameter utilized four types of flap disks with grit values ranging from #120 to #320. The 'smooth' parameter required the most extensive use of flap disks, encompassing different grit values ranging from #120 to #1200. These three parameters, 'rough,' 'medium,' and 'smooth,' exhibited varying ranges of roughness values: 1.2 – 1.4 μm, 0.6 – 0.8 μm, and 0.1 – 0.3 μm, respectively. Throughout this study, substrates with the roughness values specified in Table 1 will be referred to as 'rough,' 'medium,' and 'smooth.

Table 1. Type of grit sandpaper used in substrate preparation

No. of Grid	Surface Parameter		
	Rough	Medium	Smooth
#120	√	√	√
#180	√	√	√
#240	-	√	√
#360	-	√	√
#600	-	-	√
#800	-	-	√
#1000	-	-	√
#1200	-	-	√
Surface Roughness Value (R_a)	1.2 – 1.4 μm	0.6 – 0.8 μm	0.1 – 0.3 μm

The electrodeposition process was carried out using an electrolytic solution containing a combination of $NiSO_4$, graphene oxide, H_3BO_3, ascorbic acid, and saccharin powder in the form of chemical powder, which was dissolved in one liter of distilled water in a beaker. The composition of the compound used to produce the electrolyte is shown in Table 2.

Table 2. Bath composition

Bath Composition	
$NiSO_4$	35.04 g/L
H_3BO_3	16.48 g/L
Ascorbic Acid	11.74 g/L
Saccharin Powder	1.36 g/L
Graphene Oxide	0.05 g/L
$NiSO_4$	35.04 g/L
H_3BO_3	16.48 g/L

2.2 Electrodeposition Process Measurements

The substrate used as the cathode during the electrodeposition process was mild steel with a surface area of 1.9 x 10^3 mm^2, while the anode was composed of graphite rods with a diameter of 16 mm. The two electrodes were arranged in parallel, with 30 mm. To suspend the particles, magnetic agitation at 350 rpm was employed during electrodeposition. The coatings were fabricated using a direct current of 2A/dm^2 with a constant temperature of 45 °C and electrolyte pH of 3.0 - 3.5. The electrodeposition parameters are detailed in Table 3 and the schematic diagram of Ni-GO nanocomposite coating was shown in Figure 1.

Table 3. Electrodeposition parameter

Electrodeposition Parameter	
Temperature	45°C
Magnetic Agitation	350 rpm
Deposition Time	45 minutes
Electrolyte pH	3.0 – 3.5
Direct Current	2.00 A

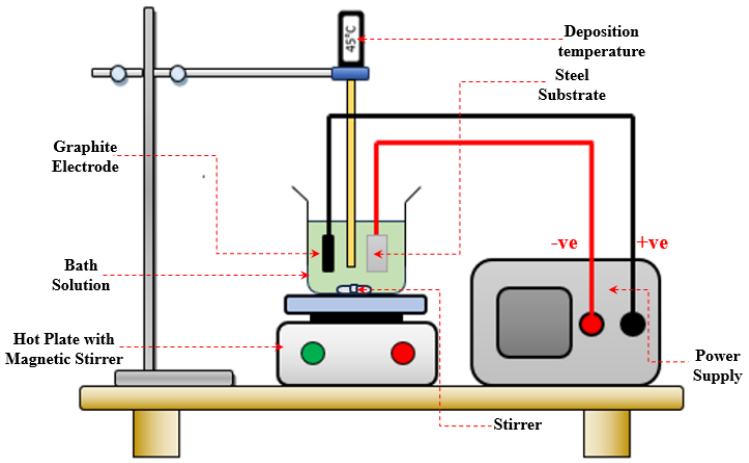

Figure 1. Schematic diagram of the electrodeposition process for Ni–GO nanocomposite coatings

2.3 Characterization Methods

The microhardness of the samples was calculated using a micro-hardness testing machine (MITUTOYO MVK-H1). A force of 9.81 N was applied for 12 seconds at three different sites, and the average value was taken as the hardness of the individual sample. The surface roughness profile of the coating samples was determined by measuring with the Alicona Infinite Focus. The roughness of the coating surface was evaluated using 5X magnification, and the average roughness was calculated by measuring three spots on the surface, each spot approximately 2.9 mm x 2.2 mm in size. The adhesive strength of the deposited layer was assessed using a micro-scratch tester (Micro Material Ltd., Wrexham, UK) with a load range of 0 - 2500 mN. Scratches were generated using a conical Rockwell diamond tip with a radius of 25 µm, which penetrated the coated surface at a constant rate of 1 µm/s under progressive loading. The adhesive strength of the coating to the substrate was determined by measuring the length of the scratch and identifying the load at which the coating completely detached from the substrate. The critical load value was confirmed by examining the scratch tracks. Additionally, the critical loads on the scratch tracks were determined for three different surface roughness conditions. The frictional curve and penetration depth were evaluated as a function of the critical load to assess the magnitude of the critical load.

Observation and elemental analysis were performed using a scanning electron microscope (SEM Hitachi SU3500) with energy-dispersive X-ray spectroscopy. The XRD machine, RIGAKU ULTIMA IV, was utilized to investigate the preferred crystallographic orientation and the average grain size of the coatings. The structural pattern, which is a characteristic of the coated particles, was analyzed. An XRD study was carried out to determine the structure of nickel and graphene in the coating, using a 2-Theta range angle between 10 and 80 and a scan rate of 4 rad/min. Confocal micro-Raman imaging (Thermo Scientific, DXR2xi) was used to examine the presence of graphene powder in the coating layer.

Slurry erosion tester machine of DUCOM TR-40, was used to conduct wear testing. The test involved a 6-hour duration with the machine rotating at 1200 rpm. The test was performed with a time interval of 2 hours. Three samples with different surface roughness parameters were subjected to testing. Silica sand with a particles size range of 125-250 μm were used in the test. The sample loss during the time interval was monitored and recorded throughout the test. Additionally, a salt spray test was performed to evaluate corrosion. The test was conducted in a closed testing chamber using pressurized air to spray a solution consisting of 5 % sodium chloride (NaCl) and distilled water. This created a corrosive environment within the chamber for 24 hours. Upon completion of the test, the specimen was inspected for corrosion, which could occur in either a larger or smaller corrosive area depending on the specimen's corrosion resistance.

3. RESULTS AND DISCUSSION

3.1 Surface Morphology of Coatings

Figures 2 (a-c) depict micrographs of coatings on rough, medium, and smooth type of surface substrates, respectively, revealing the presence of Nickel and Graphene Oxide. The spherical particles in the micrographs represent nickel, while the darker areas indicate graphene oxide deposition. The arrow in each figure points to the location of graphene oxide in the microstructure. The data from Figures 2 (a-c) indicate that the presence of graphene oxide is more prominent in the sample with a smooth substrate roughness, as shown in Figure 2(c). Additionally, it is apparent that particle agglomeration and voids are more visible in coatings on rough substrates, whereas coatings on smoother substrates exhibit uniform and smooth surfaces. The smaller particle size observed in Figure 2(c) on the smoother substrate may be attributed to reduced particle agglomeration during deposition. A smoother substrate surface facilitates a well-distributed coating deposition of fine grains hence it means that the Ni-GO nanocomposite coating is a high phosphorus-containing coating as evidenced in Figure 2(c) significantly.

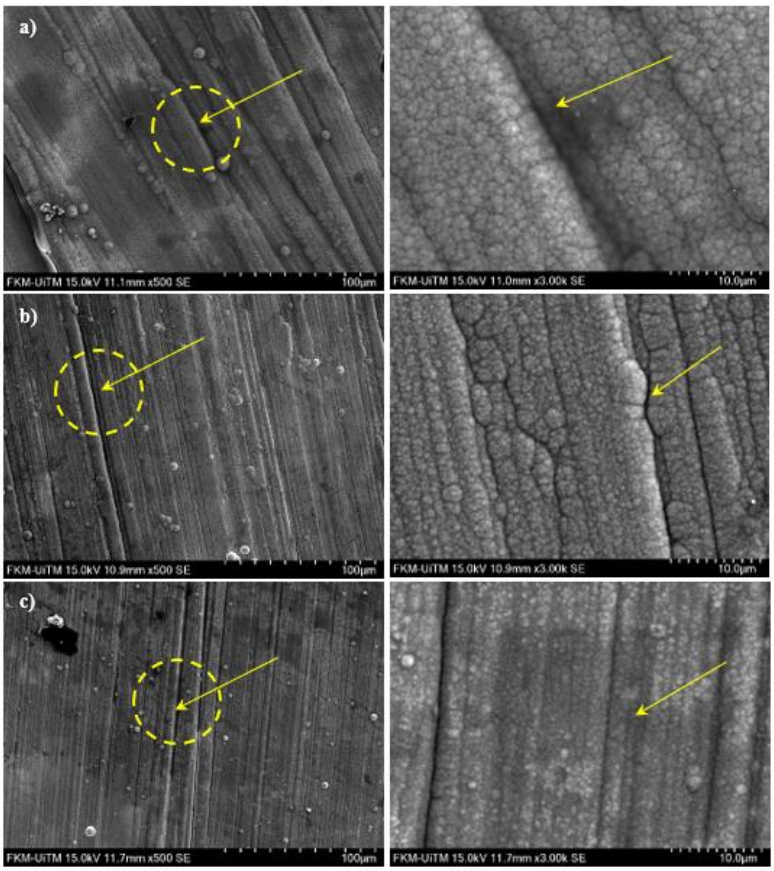

Figure 2. SEM Images: (a-c) for the surface morphologies of Ni-GO nanomposite coating prepared from rough, medium and smooth surfaces parameter with magnification of 500 (left) and 3.00k (right)

3.2 Microhardness of Coatings

Figure 3 displays the microhardness values of a coating can provide valuable information about its mechanical properties and performance. The microhardness values in the Ni-GO nanocomposite coating varied depending on the substrate surface roughness. The results showed that the microhardness of the smooth substrate specimen was the highest at 435.47 HV. In comparison, the medium surface roughness substrate had a microhardness value of 358.40 HV, and the rough surface substrate had a microhardness value of 246.33 HV. This suggests that the surface roughness of the substrate can influence the microhardness of the Ni-GO nanocomposite coating. Based on the experimentation conducted, it was observed that the microhardness values of Ni-GO nanocomposite coating varied depending on the roughness of the substrate surface. These findings suggest that the smooth substrate provides a higher microhardness value, indicating better mechanical properties and potentially improved performance of the coating [12]. This information is important as it suggests that optimizing the smoothness of the substrate surface can lead to improved mechanical properties and performance of the Ni-GO nanocomposite coating.

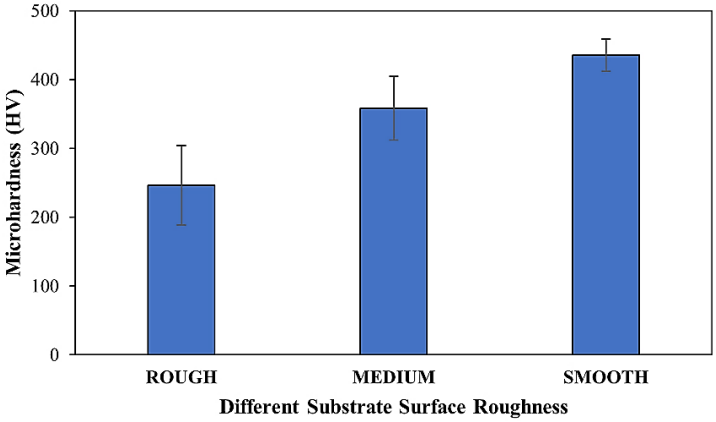

Figure 3. Vickers microhardness of different surface parameter of Ni-GO nanocomposite coating

3.3 Surface Roughness of Coatings

Next, Figure 4 shows the average Ni-GO nanocomposite coating surface roughness of rough, medium, and smooth substrate surface roughness. The specimen with the roughest substrate had the lowest average Ni-GO nanocomposite coating surface roughness value of 1.65 µm, while the specimen with a smooth substrate of Ni-GO nanocomposite coating surface roughness had the highest value of 2.11 µm. The specimen with a medium surface roughness of substrate had an intermediate surface roughness value of 1.87 µm. It can be observed that the specimen with the smooth substrate had the higher average Ni-GO nanocomposite coating surface roughness value. This observation is contradicted with previous research studies that focused on the influence of substrate roughness on coating properties. The roughness of the substrate surface can affect the adhesion and distribution of graphene oxide nanoparticles in the coating due to its applications. It is important to note, however, that the relationship between substrate roughness and coating roughness is not always straightforward. Multiple factors, such as the deposition process, particle size, and coating thickness, can also influence the resulting surface roughness of the nanocomposite coating [13].

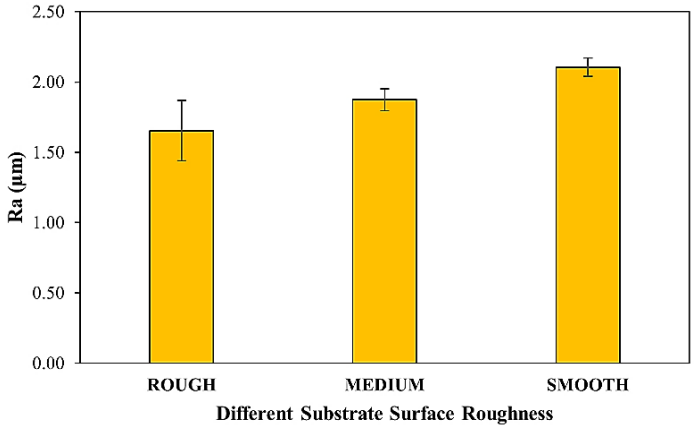

Figure 4. Surface roughness of different surface parameter of Ni-GO nanocomposite coating

Therefore, it is crucial to carefully consider all these factors and their interactions when designing and fabricating Ni-GO nanocomposite coatings. In addition to the surface roughness of the coating, other factors such as wear and corrosion resistance should also be considered when evaluating the performance of the coatings [14]. While the roughness of the substrate surface does have an impact on the resulting surface roughness of the Ni-GO nanocomposite coating, it is important to consider a general approach and consider various factors that affect the overall performance of the coating.

In conclusion, while the surface roughness of the substrate does play a role in determining the surface roughness of the Ni-GO nanocomposite coating, it is just one of many factors that can influence the overall functionality and performance of the coating.

3.4 Crystallite Structure of Deposited Coatings

Next, to obtain the crystallite structure from XRD spectra of the coating on the specimen, the 2-Theta angle was set up at 10 to 80 radiations. Figure 5 displays the XRD Pattern of Ni-GO nanocomposite coating for three different types of substrate surface roughness. The XRD spectra of all coatings exhibited the characteristic peak of the face-centered-cubic crystalline structure. Moreover, as shown in Figure 5, the intensity decreases as the roughness value decreases. Figure 5(a) displays an overlap between Graphene and Nickel at 44.7, while in Figure 5(b), the overlap between nickel and graphene occurs at 44.8 and 76.6. In Figure 5(c), the overlap between graphene and nickel can be observed at 44.8 and 52.1. The XRD analysis allows to study the atomic and molecular arrangement within a material by analyzing the scattering pattern produced when a beam of X-rays interacts with the crystal lattice of the material. In the case of the Ni-GO nanocomposite coating, the XRD analysis was performed to identify the presence and characteristics of the crystalline structure. The XRD spectra of all coatings exhibited the characteristic peak of the face-centered-cubic crystalline structure, indicating that the coating has a well-defined and ordered arrangement of atoms. Furthermore, it was observed that the intensity of the XRD peaks decreases as the surface roughness of the substrate decreases. This suggests that the coating is more evenly deposited on a rougher substrate surface compared to a smoother one This suggests that the crystalline structure of the coating is influenced by the roughness of the substrate [15]. The XRD analysis also revealed an overlap between the peaks corresponding to graphene and nickel in the coating. This indicates that the graphene and nickel components are present in the coating and are interacting with each other.

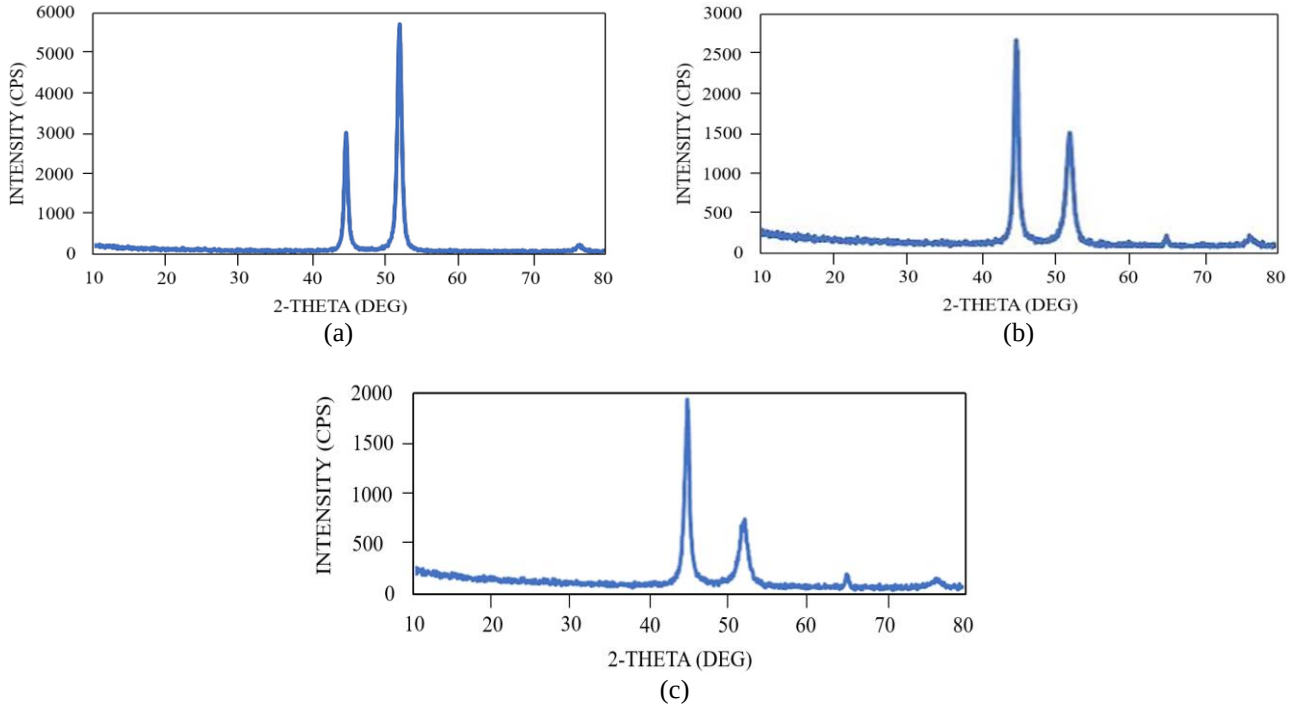

Figure 5. The XRD pattern of Ni-GO nanocomposite coating on: (a) Rough roughness substrate, (b) Medium roughness substrate and (c) Smooth roughness substrate

3.5 Raman Spectra of Coatings

Raman spectra are typically employed to describe a material's structural properties, such as the degree of internal disorder, defect density, and element doping. A carbon substance known as graphene has a sp2-hybridized structure. The d-peak and G-peak are the distinctive peaks of the Raman spectra of graphene. The integrated intensity ratio of the D-band and G-band is R (ID/IG). The rough substrate structure has a high integrity when R is high. The largest D-peak among them demonstrates the high disorder with huge values and the lattice defects of graphene carbon atoms in smooth substrate occur at approximately 1347 cm^{-1}. The phonon scattering of the sp2 carbon atom results in the G-peak, the distinctive peak of graphene. It often appears between 1605 cm^{-1} (G) and 3006 cm^{-1} (2D), which denotes carbon that has undergone sp2 hybridization. The distinct peak may be an indication of the orderly and full graphene structure in smooth roughness. The Raman shifts of graphene following oxidation-reduction is shown in Figure 6. The graphene diffraction peak is located at 1601 cm^{-1} and 1608 cm^{-1} (G), respectively, and is moved to the medium and rough roughness diffraction peak at 1346 cm^{-1} and 1343 cm^{-1} (D). The diffraction peak of graphene in smooth shifts to the peak of graphene in two dimensions at 3006 cm^{-1}, and the peak strength falls as the peak breadth increases. Due to the tiny size effect and growing specific surface area of graphene, which could result in several new chemical vibration bonds, the 2D is migrating to the right and becoming wider subsequently [16].

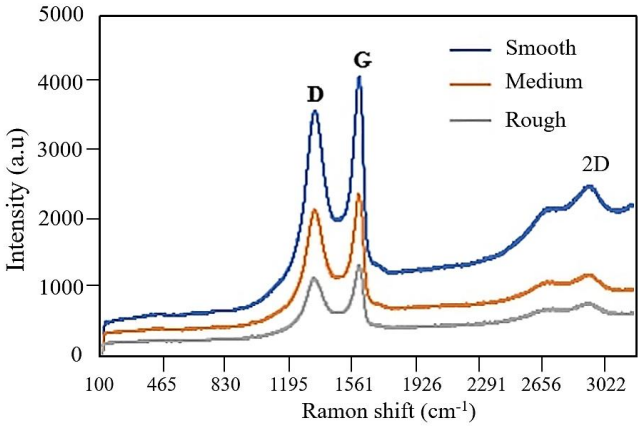

Figure 6. Raman spectra for Ni-GO nanocomposite coating of three different substrates surface roughness

3.6 Adhesion Strength of Coatings

In this investigation, the adhesion strength of the coating layer to the substrates was assessed using the scratch test, which is a commonly used technique for evaluating adhesion. However, there is currently no standardized process for qualitative assessment of adhesion strength. It is important to note that several intrinsic and extrinsic factors, including scratch speed, indenter shape, loading rate, surface condition, substrate and coating properties, test environment, and friction coefficient, can influence the critical load value, which represents the point at which the coating separates from the substrate [17,18]. Micrographics illustration of the critical loads and crack failure along the scratch track of the coating in three different substrate surfaces are shown in Figure 7(a) to (c) respectively. The critical load for each scratch track profile was determined under varying substrate surface roughness and scanning distances, and the results were presented in the similar figure. A load of 2500 mN was applied, and the total length of the scratch track was 1000 μm. Initially, the coating layer exhibited an elastic-plastic transition state, with more indenter penetration into the coating layers as the applied load gradually increased.

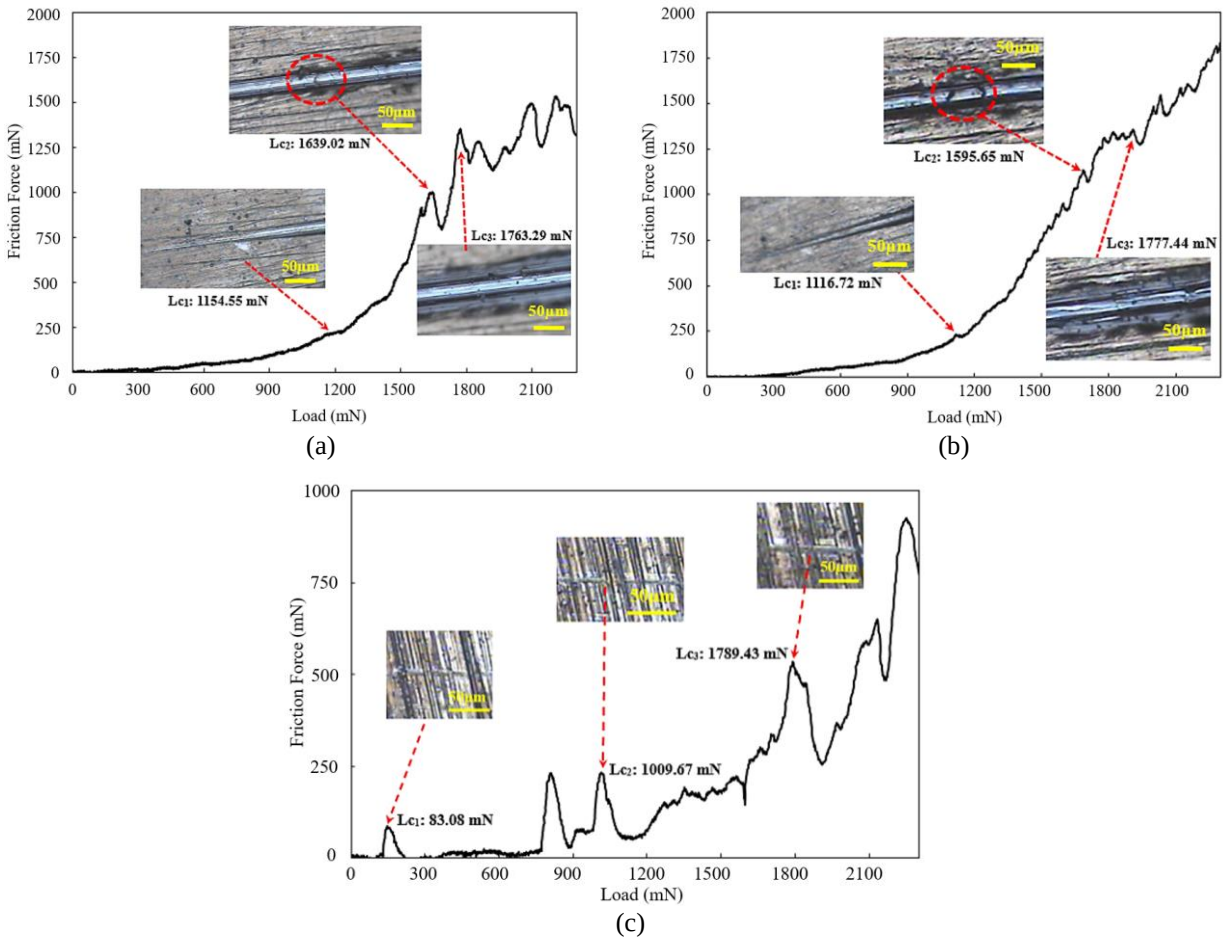

Figure 7. Load and crack failure along scratch track of: (a) Smooth substrate surface, (b) Medium substrate surface and (c) Rough substrate surface Ni-GO nanocomposite coatings

Based on the information illustrated in Figure 7, the loads applied, and crack failures were documented during a scratch test performed on a Ni-GO nanocomposite coating across three distinct levels of substrate surface roughness. The scratch test entailed a left-to-right direction on all coatings, and critical loads were ascertained by examining alterations in the depth profile and acoustic emission linked to coating delamination [19]. Three critical loads Lc_1 (adhesive failure), Lc_2 (adhesive and cohesive failure), and Lc_3 (total coating failure) were established. Notably, the coating on a smooth substrate surface displayed a noteworthy accumulation of debris along the wear track, with adhesive failure occurring at a low critical load, Lc_1 = 1154.6 mN. Conversely, a complete delamination of the smooth substrate surface at a critical load of Lc_2 = 1639.0 mN resulted in cohesive failure with chipping on both sides of the scratch track. The medium roughness of the substrate surface exhibited a similar scratch pattern, with adhesive failure at Lc_1 = 1116.7 mN. In contrast, the rough surface substrate displayed distinct failure shapes, failing earlier than other substrate roughness levels, with a critical load of Lc_2 = 83.1 mN. The highest adhesive strength among the three samples was observed in the sample with the smoothest substrate surface, manifesting total coating failure at a critical load of Lc_3 = 1761.2 mN. The reduction in critical load could potentially be attributed to the heightened residual stress generated during the thermomechanical reactions occurring in the coating process. Consequently, adhesive strength tends to decrease with increasing levels of residual stress in the medium roughness of the substrate surface. Residual stresses can hinder the adhesion of coatings to substrate surfaces, resulting in reduced adhesive strength. High levels of residual stress can introduce internal forces within the material, which can exceed the adhesive bond strength and cause delamination or cracking. Furthermore, residual stress can also affect the cohesive strength of the material itself, leading to a decrease in overall mechanical properties [20]. These effects on adhesion and mechanical properties can have destructive consequences for the performance and durability of coatings in various applications. Therefore, it is important to carefully consider and control the residual stresses during the coating process to ensure optimal adhesive strength.

3.7 Slurry Erosion Test

The wear performance resistance of the coating was assessed using DUCON TR-40. The test involved utilizing silica sand with a particle size of 125-250 μm at a rotation speed of 1200 rpm. The weight loss of the specimens for each parameter is presented in Figure 8. This figure presents a graph depicting the weight reduction for each parameter during the slurry erosion test. The graph reveals that rough surfaces experienced more weight loss compared to medium and smooth samples. It can be observed that all coatings underwent a slight weight loss during the process, which is attributed to the increase in erosion rate over time [21, 22]. The slopes of the smooth and medium graphs are nearly flat, while the rough graph is slightly steeper in comparison to both other parameters. This indicates that rough surfaces exhibited lower resistance to wear when compared to medium and smooth surfaces, as also supported by Figure 9(a) and Figure 9(b). Figure 9(a) displays the total weight loss for each parameter, where smooth surfaces only experienced a loss of 0.102 g, while rough surfaces showed the highest weight loss of 0.197 g, with a difference of 0.095 g compared to smooth surfaces. On the other hand, medium surfaces exhibited a weight loss of 0.129g, with a difference of 0.027 g compared to smooth surfaces. According to Figure 9(b), the percentage weight loss for rough surfaces was the highest at 0.362 %, compared to medium and smooth surfaces, which experienced weight losses of only 0.249 % and 0.182 %, respectively. Based on the results, it was observed that rough surfaces experienced higher weight loss compared to medium and smooth surfaces. This indicates that rough surfaces are more inclined to wear and may require additional protective measures. These findings suggest that surface roughness plays a crucial role in determining the wear performance of coatings [23]. Additionally, Figure 9 (a) and (b) depicting the weight reduction for each parameter during the slurry erosion test showed that all coatings underwent a slight weight loss over time. This weight loss is attributed to the increase in erosion rate, indicating that even the most resilient coatings will experience some wear over time.

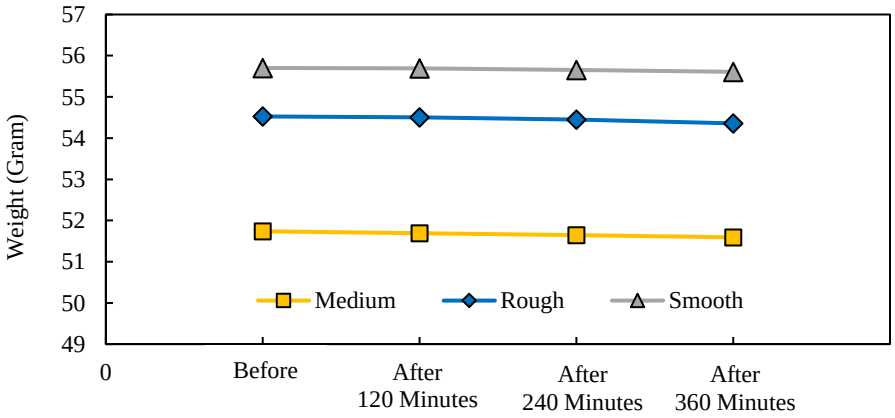

Figure 8. Weight reduced for each substrate roughness during the slurry erosion test

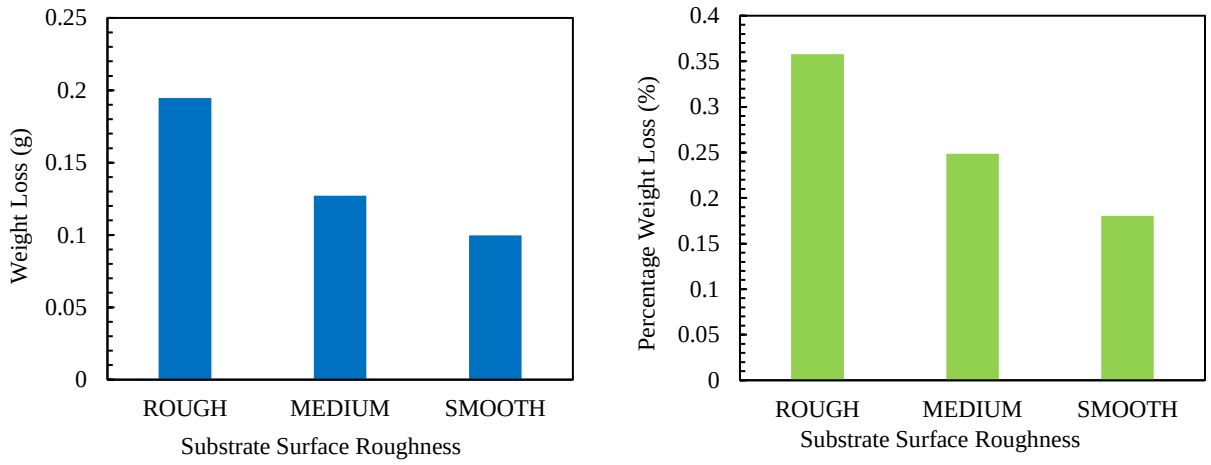

(a) (b)

Figure 9. (a) Total weight loss for each substrate surface roughness and (b) Percentage weight loss for each substrate surface roughness

3.8 Corrosion Test

The effectiveness of substrate surface roughness on Ni-Graphene coating to withstand corrosion was tested using a salt spray test. Figure 12 shows the results of weight gain after the salt spray test. The weight gained on the specimen is due to the formation of an oxide layer during the salt spray process. Based on the results in Figure 10, the specimen with a rougher substrate showed the highest weight gain of 0.0524 g, while the specimen with a smoother substrate had the lowest weight gain of 0.0189 g. From the results, it is evident that the corrosion rate decreases as the surface roughness of the coating increases. One important factor that influences the corrosion rate is the roughness of the coating which may hugely be influenced by the surface roughness of substrate. Ghosh and team suggested that coatings with rough surfaces exhibit higher resistance to wear and corrosion compared to those with smooth surfaces [24]. This phenomenon can be attributed to several factors. Rough coating surface provides more areas of contact between the coating and the corrosive environment. This increased contact area which allow more effective diffusion of corrosive agents, leading to a decrease of the corrosion rate. Additionally, the roughness of the coating surface can also promote the formation of protective oxide layers [25]. These oxide layers act as barriers, preventing further corrosion of the underlying material. Furthermore, the roughness of the coating surface can also enhance the adhesion between the coating and the substrate material. This helps to prevent the penetration and diffusion of corrosive agents, thereby reducing the corrosion rate.

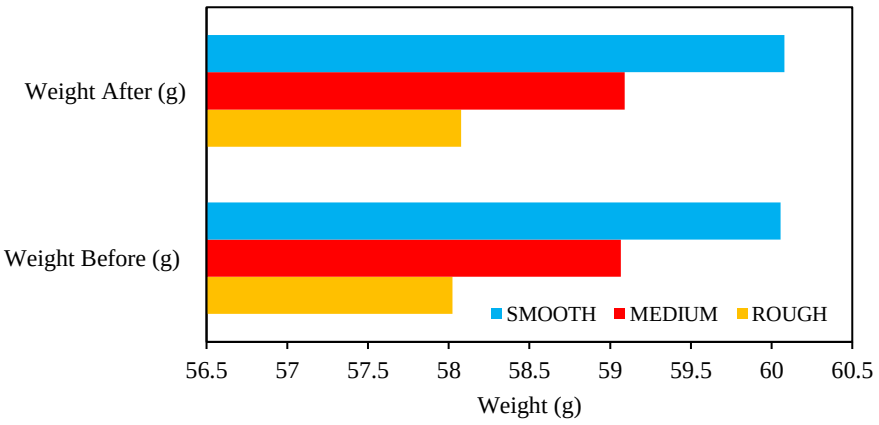

Figure 10. Weight addition of each substrate surface roughness before and after the salt spray test

4. CONCLUSION

In this study, the effect of substrate surface roughness on the corrosion and wear rate of Ni-GO nanocomposite coating was successfully studied and investigated. It was found that smooth substrate surfaces exhibit effective results in microhardness and the surface roughness of the coating. The crystallite structure results in XRD patterns show the incorporation of GO in the Ni-matrix, appearing at the similar peak of 200. The adhesion strength of the Ni-GO nanocomposite coating was enhanced when deposited on smooth substrate. The Ni-GO nanocomposite coating on smooth substrate surfaces disclosed a reduced wear rate and improved corrosion resistance. Therefore, the results obtained in this study support the possibility of improving the tribological performance of the coating through the remarkable functionality of GO with proper substrate preparation of polishing.

5. ACKNOWLEDGMENT

The authors would like to thank Universiti Teknologi MARA (UiTM) Shah Alam for the facilities and equipment provided for this project. This work was supported by UiTM Research Intensive Grant 600-RMC/GIP 5/3 (2022).

6. REFERENCES

[1] P. Natarajan, A. Jegan, S. Sankar Ganesh, "Development of numerical model for predicting the characteristics of Ni–SiC nano composite coatings on AISI 1022 substrate," *Material Research Express*, vol. 6, no. 8, p. 085048, 2019.

[2] W. Ayoola, S. Durowaye, K. Andem, O. Oyerinde, J. Ojakoya, "Effects of surface preparation on the corrosion behavior of mild steel," *Tikrit Journal of Engineering Sciences*, vol. 29, no. 1, pp. 16–25, 2022.

[3] P. Yu, Y. Lei, Z. Luan, Y. Zhao, H. Peng, "Effect on the surface anticorrosion and corrosion protection mechanism of integrated rust conversion coating for enhanced corrosion protection," *ACS Omega*, vol. 7, no. 10, pp. 8995–9003, 2022.

[4] Y. I. Kuznetsov, G. V. Redkina, "Thin protective coatings on metals formed by organic corrosion inhibitors in neutral media," *Coatings*, vol. 12, no. 2, p. 149, 2022.

[5] X. Li, Q. Shen, Y. Zhang, L. Wang, C. Nie, "Wear behavior of electrodeposited nickel/graphene composite coating," *Diamond and Related Materials*, vol. 119, p. 108589, 2021.

[6] C. Liu, D. Wei, X. Huang, Y. Mai, "Electrodeposition of Co-Ni-P graphene oxide composite coating with enhanced wear and corrosion resistance," *Journal of Materials Research*, vol. 34, no. 10, pp. 1726–1733, 2019.

[7] Y. Raghupathy, A. Kamboj, M. Y. Rekha, N. P. Narasimha Rao, C. Srivastava, "Copper-graphene oxide composite coatings for corrosion protection of mild steel in 3.5 % NaCl," *Thin Solid Films*, vol. 636, pp. 107–115, 2017.

[8] Z. Duan, "Application of graphene in metal corrosion protection," *IOP Conference Series: Materials Science and Engineering*, vol. 493, no. 1, 2019.

[9] L. Xiang, Q. Shen, Y. Zhang, W. Bai, C. Nie, "One-step electrodeposited Ni-graphene composite coating with excellent tribological properties," *Surface and Coatings Technology*, vol. 373, pp. 38–46, 2019.

[10] X. H. Zhang, X. X. Li, W. J. Liu, Y. Q. Fan, H. Chen, T. X. Liang, "Preparation and tribological behavior of electrodeposited Ni–W–GO composite coatings," *Rare Metals*, vol. 38, no. 7, pp. 695–703, 2019.

[11] R. Jiang, X. Zhou, Z. Liu, "Electroless Ni-plated graphene for tensile strength enhancement of copper," *Materials Science and Engineering A*, vol. 679, pp. 323–328, 2017.

[12] Y. Wang, W. Gao, "Microstructure and performance of Ni/TiN coatings deposited by laser melting deposition on 40Cr substrates," *Coatings*, vol. 12, no. 3, p. 367, 2022.

[13] M. B. Hegde, K. N. Mohana, "A sustainable and eco-friendly polymer based graphene oxide nanocomposite anti-corrosion coating on mild steel," *ChemistrySelect*, vol. 5, no. 4, pp. 1506–1515, 2020.

[14] S. A. N. Mehrabani, R. Ahmadzadeh, N. Abdian, A. T. Tabrizi, H. Aghajani, "Synthesis of Ni-GO nanocomposite coatings: corrosion evaluation," *Surfaces and Interfaces*, vol. 20, p. 100546, 2020.

[15] X. Shi, J. Wang, L. Gong, H. Luo, "Investigation of the antifouling mechanism of electroless nickel-phosphorus coating against sand and bitumen," *Energy and Fuels*, vol. 33, no. 7, pp. 6350–6360, 2019.

[16] F. Zhong, Y. He, P. Wang, C. Chen, Y. Lin, Y. Wu, et al., "Self-assembled graphene oxide-graphene hybrids for enhancing the corrosion resistance of waterborne epoxy coating," *Applied Surface Science*, vol. 488, pp. 801–812, 2019.

[17] M. A. Hassan, A. R. Bushroa, R. Mahmoodian, "Identification of critical load for scratch adhesion strength of nitride-based thin films using wavelet analysis and a proposed analytical model," *Surface and Coatings Technology*, vol. 277, pp. 216–221, 2015.

[18] Y. F. M. Yunos, M. Y. Ibrahim, "Mechanical properties (scratch test) of silicanizing process on mild steel substrate using tronoh silica sand," *Jurnal Tribologi*, vol. 26, pp. 60–67, 2020.

[19] N. Schwarzer, Q.-H. Duong, N. Bierwisch, G. Favaro, M. Fuchs, P. Kempe, et al., "Optimization of the scratch test for specific coating designs," *Surface and Coatings Technology*, vol. 206, no. 6, pp. 1327–1335, 2011.

[20] M. Abdoos, B. Bose, S. Rawal, A. F. M. Arif, S. C. Veldhuis, "The influence of residual stress on the properties and performance of thick TiAlN multilayer coating during dry turning of compacted graphite iron," *Wear*, vol. 454–455, p. 203342, 2020.

[21] S. A. Aldahash, O. Abdelaal, Y. Abdelrhman, "Slurry erosion-corrosion characteristics of as-built Ti-6Al-4V manufactured by selective laser melting," *Materials (Basel)*, vol. 13, no. 18, p. 3967, 2020.

[22] X. Zhu, Y. Zhao, L. Ma, G. Zhang, W. Ren, X. Peng, et al., "Graphene coating makes copper more resistant to plastic deformation," *Composites Communications*, vol. 12, pp. 106–111, 2019.

[23] Z. Tu, E. Hu, B. Wang, K. D. David, P. Seeger, M. Moneke, et al., "Tribological behaviors of Ni-modified citric acid carbon quantum dot particles as a green additive in polyethylene glycol," *Friction*, vol. 8, no. 1, pp. 182–197, 2020.

[24] R. Ghosh, V. Sudha, S. Harinipriya, "Thermodynamic analysis of electrodeposition of copper from copper sulphate," *Bulletin of Materials Science*, vol. 42, no. 2, pp. 1–8, 2019.

[25] R. Ding, W. Li, X. Wang, T. Gui, B. Li, P. Han, et al., "A brief review of corrosion protective films and coatings based on graphene and graphene oxide," *Journal of Alloys and Compounds*, vol. 764, pp. 1039-1055, 2018.